

RESULTS FROM CDF AND DØ (EVERYTHING BUT THE *B*)

Harold G. Evans*

Physics Dept., Columbia University

MailCode 5215

538 W. 120th St., New York, NY 10027

Representing the CDF and DØ Collaborations

ABSTRACT

With the start of Run II at the Fermilab Tevatron a host of new physics opportunities are opened. In this paper we will review the prospects for physics at the CDF and DØ experiments. Topics ranging from QCD, to electro-weak precision measurements, to top-quark physics, to searches for the Higgs boson and signals of physics beyond the Standard Model will be discussed. B-Physics at the Tevatron is covered in a separate contribution to these proceedings. We will outline how upgrades to the accelerator and the detectors make these studies possible with precisions higher than ever achieved previously and will show results from the first data collected in Run II. These results give us confidence in our ability to achieve ambitious physics goals, and point the way toward a bright future for the Tevatron.

1 Introduction

“High energy physics is a particularly exciting field right now.” We have all heard that statement so many times that it has begun to ring rather desperately in our ears. In this case, however, the Bellman is right.¹ We *are* on the verge of making fundamental advances in our understanding of questions that are of interest even to our non-physicist friends. Why is there mass and how does it arise? Why isn’t there more antimatter? How is matter put together? None of these questions are addressed by the current Standard Model of particle interactions (SM) although, up to now, it has succeeded in accurately predicting thousands of experimental measurements² (with the exception of finite neutrino masses).

Within the next decade, this situation will almost certainly change. Our understanding of the mechanism of mass generation, which, in the SM, is tied up with the breaking of symmetry between electro-magnetic and weak interactions, will take a huge stride forward with the discovery (or exclusion altogether) of the Higgs boson, the only inhabitant of the SM zoo yet to be observed. Will this elusive particle have all the properties predicted by the SM? Or will its characteristics fit better with those predicted by extensions of the SM? Perhaps it doesn’t exist at all and some other mechanism will be found to break the electro-weak symmetry?

Answering these questions definitively is within the grasp of experiments now running or being built. It will require a multi-prong strategy though, with direct searches for Higgs-like particles being complemented with predictions of the Higgs properties using precision measurements of other electro-weak parameters (for example, the W -boson and top-quark masses) and measurements of rare decays (especially those of heavy particles such as τ , b and t).

Electro-weak symmetry breaking is not the only phenomenon that should yield secrets in the coming years. The overwhelming preponderance of matter in the observable universe is an effect that is intimately connected with the violation of CP symmetry. All indications are that the CP violation present in the Standard Model is not sufficient to explain the observed asymmetry between matter and antimatter.³ However, sources of CP violation beyond those in the SM may well contribute here. Studies of B -hadron and kaon properties as well as neutrino oscillations are crucial to this understanding, and again, experiments taking data now or in the near future should clarify this question substantially.

Finally, knowing how the masses of quarks, leptons and bosons arise and the link

between this process and electro-weak symmetry breaking still does not tell us why the proton has the mass it does. To understand this, we must understand the intricacies of the strong interaction. This has been a long process for which important information will be gathered in the experiments running over the next few years.

Looking over this list of fundamental questions it's easy to see why the Fermilab Tevatron will be a focal point of high energy physics for years to come. After a successful data taking period from 1992–1996 (Run I), which saw, among other things, the discovery of the top quark,⁴ the Tevatron started a new era of data taking in March 2001 (Run II). In Run II proton-antiproton collisions occur in the CDF and DØ detectors at a center of mass energy of 1.96 TeV, which represents the highest energy available at a collider. We can use these interactions to study all of the questions above: from direct Higgs searches and searches for particles beyond those predicted in the SM, to precision measurements of SM parameters, to studies of B-physics and CP violations, to sensitive probes of the strong force and its theory, quantum-chromodynamics (QCD). As you will see, these studies are expected to be consistently among the most sensitive available with a real chance of finding something truly groundbreaking. To understand why, we will walk through the physics of Run II, with the exception of B-physics, which is discussed separately in these proceedings.⁵ We'll start with a brief discussion of the Tevatron accelerator and the CDF and DØ detectors, especially comparing expected detector performances. We'll then see how these detectors are used to dig out physics signals from the large background present at a $p\bar{p}$ collider. And finally, we'll end with a brief summary of some of the most interesting physics topics of Run II, with predictions of expected sensitivities and indications from the first data collected as to how the detectors are actually performing. Unfortunately, space limitations preclude the discussion of interesting results still coming from Run I data of the Tevatron. So, with an eye toward the future – let's get started.

2 Run II at Fermilab

2.1 The Tevatron

The Fermilab Tevatron accelerator facility has been substantially modified to achieve the high luminosities required by the physics goals of Run II, which began officially in March of 2001. The main changes with respect to previous Tevatron running are in the center-of-mass energy of the $p\bar{p}$ collisions, which has been increased from 1.8 TeV

to 1.96 TeV between Runs I and II, and in the instantaneous luminosity, which should increase by more than two orders of magnitude with respect to the values achieved in Run I. Some of the factors contributing to these changes are detailed in Table 1 (see Ref. 6).

Because of these accelerator changes physics prospects at Run II are improved in two ways. Obviously, the increase in the amount of data available made possible by increased Run II luminosities will allow new analyses to be performed and will increase the statistical precision of old ones. However, the small increase in CM energy over Run I actually results in a substantial increase in cross-section for several interesting physics channels. For example, cross-sections for W/Z , top quarks and jets with $P_t > 400$ GeV will increase by factors of 1.1, 1.35 and 2, respectively.

By July, 2002 the Tevatron had delivered approximately 50 pb^{-1} of data to CDF and DØ. Of this data the experiments recorded $10\text{--}20 \text{ pb}^{-1}$, which was used to produce the results presented at the ICHEP02 conference in Amsterdam⁷ upon which this paper is based. In the future, Run II data taking is foreseen to happen in two main stages – Run IIa, where approximately 2 fb^{-1} of data will be collected, and Run IIb, where a total integrated luminosity of $10\text{--}15 \text{ fb}^{-1}$ is hoped for. The exact timing of the transition between Runs IIa and IIb will be determined by degradation of the CDF and DØ silicon detectors with radiation dose accumulated and is expected to occur around 2005-2006. Details of the machine goals for Runs IIa and IIb are given in Table 1.

Table 1. A comparison of the Run I and Run II parameters at the Fermilab Tevatron.

	Run Ib typical	Run IIa → July 02 goal		Run IIb goal
Years	92–96	01–05		06–LHC
E_{CM} [TeV]	1.8	1.96	1.96	1.96
Bunches ($p \times \bar{p}$)	6×6	36×36	36×36	$36 \times 36(140 \times 103)$
Bunch Spacing [ns]	3500	396	396	396(132)
Total protons ($\times 10^{12}$)	1.4		9.7	9.7(38)
Total anti-protons ($\times 10^{12}$)	0.3		1.1	3.4(9.6)
<Interac's/X'ing>	2.5	<1	2.3	5.5(3.7)
Inst. Lumi. ($\times 10^{32} \text{ cm}^{-2}\text{s}^{-1}$)	0.16	0.2	0.86	2.0(4.1)
Integ. Lumi [fb^{-1}]	0.125	0.01	2	15

2.2 The Detectors

To take full advantage of the physics possibilities in Run II, both the CDF and DØ collaborations have made major upgrades to their detectors.^{8,9}

CDF has replaced their Run I silicon detector with a new device providing 3D tracking up to $|\eta| < 2$.^{*} Further improvements in tracking come from a new, faster drift chamber with 96 layers (COT) and new Time-of-Flight (TOF) detector. They have also significantly enhanced their capabilities in the forward region with a new plug calorimeter and a new forward muon system. Finally, they have upgraded their trigger system and added a new track trigger at Level-1, based on information from their drift chamber as well as constructing a new impact parameter trigger at Level-2 using data from their silicon detector. A cut-away view of the CDF Run II detector is shown in Figure 1.

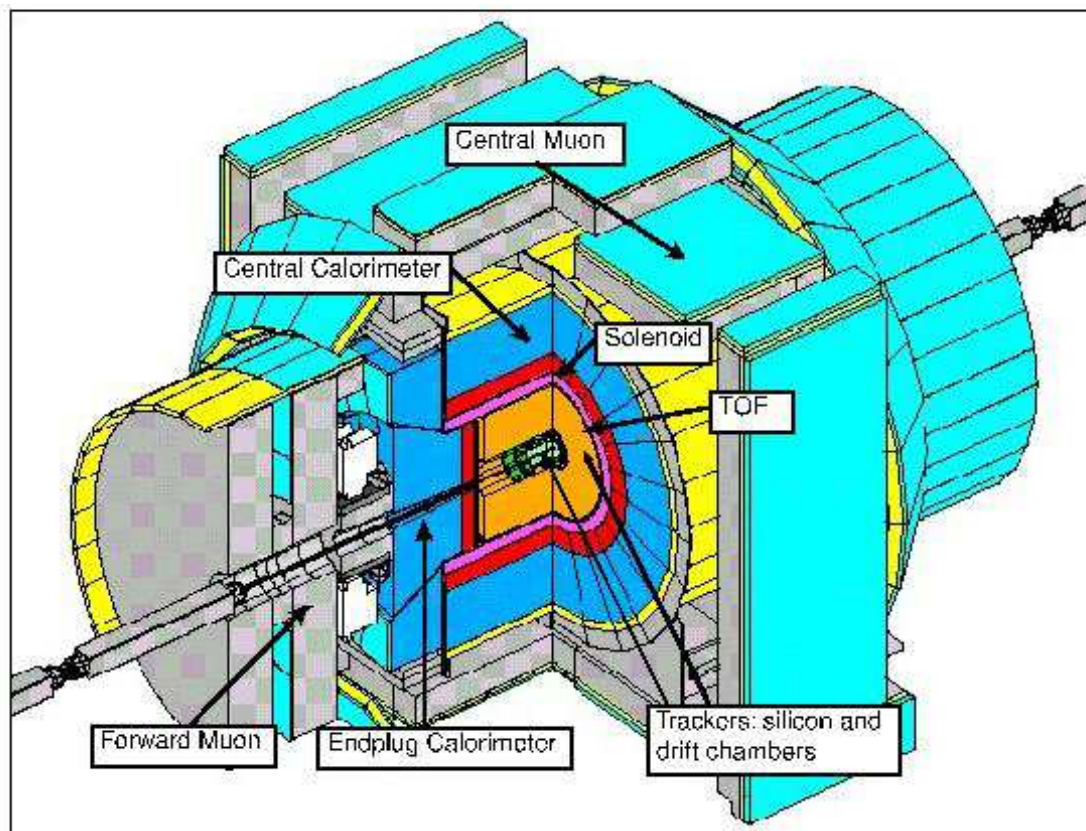


Fig. 1. The CDF Run II detector.

The DØ upgrade was also an ambitious project. The old, non-magnetic tracking

^{*}The pseudo-rapidity is defined as $\eta \equiv -\ln \tan(\theta/2)$.

system was completely replaced and now includes a silicon micro-vertex detector with 3D readout and a central tracker (CFT) using 8 super-layers of scintillating fibers immersed in a 2.0 Tesla axial magnetic field. Because of the increased amount of material in the tracking system, pre-shower detectors have been added in the central and forward regions. The $D\emptyset$ uranium-liquid argon calorimeter has been retained, but its readout electronics have been completely replaced. The muon system in the central region is also largely unchanged from Run I. However, trigger scintillator counters have been added and the muon system in the forward region has been completely replaced. Finally, totally new trigger and data acquisition systems have been installed. A diagram of the $D\emptyset$ Run II detector is shown in Figure 2.

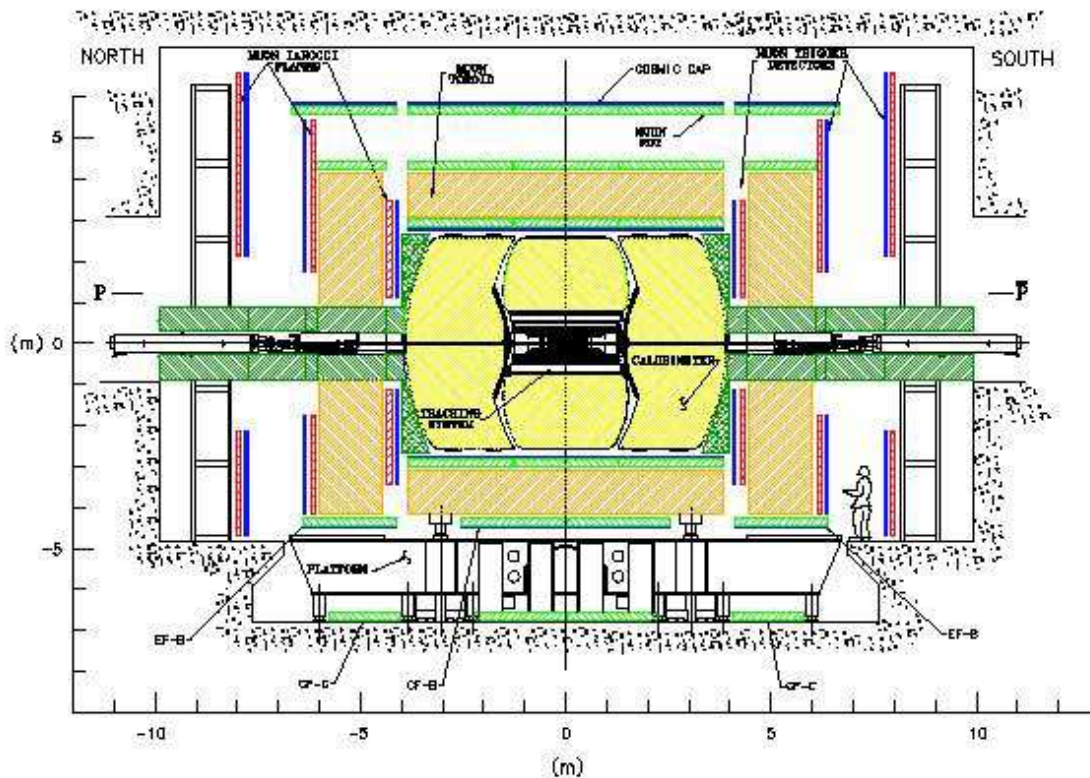


Fig. 2. The $D\emptyset$ Run II detector.

Both detectors are now operating quite well, with only some aspects of the $D\emptyset$ trigger system remaining to be commissioned. Detector performance is now approaching design goals for many of the sub-systems. A summary of some of the performance goals in Run II is given in Table 2. As can be seen, the detectors have been built to the highest standards and are expected to have largely similar capabilities. Several dif-

ferences are worth mentioning, however, as they highlight the differences in many of the analyses that will be performed by the collaborations. It should be emphasized that these performance differences tend to be rather small with both experiments expected to be able to measure a large range of phenomena with similar precision.

One of CDF's main strengths is their superb tracking system. Their excellent momentum and vertex reconstruction resolution give them an advantage in several areas of B-physics where final states must be reconstructed using several relatively low momentum tracks. DØ, on the other hand, has very strong calorimetry and muon detection covering a larger solid angle than CDF's. This is especially helpful in some analyses of physics beyond the standard model where muon, electron and jet acceptances are important. Finally, CDF and DØ have substantial differences in the philosophy of their trigger systems. While both experiments use a three-level trigger, with the first level using custom hardware, the second using special purpose CPUs and the third using a farm of PCs, an important difference can be found at level-1. Mainly because of the choice of the silicon detector readout chip, CDF can issue level-1 accepts at rates up to 50 kHz, while the DØ level-1 system is limited to approximately 5 kHz. The main consequence of this difference is that CDF can construct a low- P_t track trigger aimed at such B-physics topics as $\sin 2\alpha$ and B_s mixing using fully hadronic decays. This extended level-1 rate capability is not expected to give much advantage in such high- P_t topics as vector bosons, top and Higgs physics and physics beyond the standard model, though, since signal rates here are already quite low.

Finally, a word about coordinate systems. Both CDF and DØ use coordinate systems with the z -axis pointing along the proton beam direction, the x -axis away from the center of the ring and the y -axis pointing up. Azimuthal angles (in the $x - y$, or transverse plane) are generally denoted as ϕ , with r measuring the distance from the beam line in this transverse plane. The polar angle, θ , is measured from the z -axis and pseudo-rapidity, η , is defined using it, as described above.

3 Physics and How to Find It

Physics of interest in proton-antiproton interactions at the Tevatron comes from the "hard scattering" of a pair of (anti)quarks or gluons that make up the p and \bar{p} . Because of the large strong coupling constant, this hard scattering is governed almost exclusively by QCD, which is well-understood at these energies, and generally results in the production of light quarks or gluons with subsequent gluon radiation. These final-state

Table 2. A comparison of expected DØ and CDF detector performances in Run II.

		DØ	CDF
Tracking System			
Technologies		silicon, scintillating fibers	silicon, drift chambers
Magnetic Field	[T]	2.0	1.4
$ \eta $ accept.		$<3.0(\text{Si}), <1.7(\text{CFT})$	$<2.0(\text{Si}), <1.0(\text{COT})$
Radii	[cm]	2.8–10.0(Si), $<52(\text{CFT})$	1.6–10.7(Si), $<132(\text{COT})$
$\delta P_t/P_t$	[%]	$2 \oplus 0.2P_t$	$0.7 \oplus 0.1P_t$
Impact param res	[μm]	$13 \oplus 50/P_t$	$6 \oplus 22/P_t$
Primary vtx res	[μm]	$15\text{--}30(r - \phi)$	$10\text{--}35(r - \phi)$
Secondary vtx res	[μm]	$40(r - \phi), 80(r - z)$	$14(r - \phi), 50(r - z)$
Mass res $J/\psi \rightarrow \mu^+ \mu^-$	[MeV]	27	15
Particle ID		pre-shower	dE/dx, TOF
Calorimetry			
Technologies		uranium-liquid Ar	lead-scint./prop.-chambers
$ \eta $ accept.		<4.0	<3.6
Granularity	$(\eta \times \phi)$	0.1×0.1	0.1×0.26
EM res.	[%]	$14/\sqrt{E}$	$16/\sqrt{E}$
Jet res.	[%]	$80/\sqrt{E}$	$80/\sqrt{E}$
Muon System			
Technologies		drift tubes, scintillator	drift chamb's, scintillator
Magnetic Field	[T]	1.8	0 (central)
$ \eta $ accept.		<2.0	<1.5
ϕ coverage	[%]	>90	>80
Shielding	int. len.	12–18	5.5–20
Standalone $\delta P_t/P_t$	[%]	$18 \oplus 0.3P$	—
Trigger System			
Hardware	L1	custom electronics	custom electronics
	L2	custom CPUs	custom CPUs
	L3	PC farm	PC farm
Accept rate	L1 [Hz]	5000	50000
	L2 [Hz]	1000	300
	L3 [Hz]	50	50

Table 3. Cross-sections, rates (at $\mathcal{L} = 2 \times 10^{32} \text{ cm}^{-2}\text{s}^{-1}$), and event characteristics of various physics processes at the Tevatron in Run II.

Mode	X-Sect	Rate	$\langle E_t^{\text{jet}} \rangle$ [GeV]	$\langle E_t^{\text{lept}} \rangle$ [GeV]	$\langle ME_t \rangle$ [GeV]	Displ. V. [mm]
Inelastic $p\bar{p}$	50 mb	10 MHz	low	none	~ 0	none
$p\bar{p} \rightarrow b\bar{b}$ ($ \eta < 1$)	$50 \mu\text{b}$	10 kHz	~ 6	~ 1	~ 0	few
$p\bar{p} \rightarrow WX \rightarrow \ell\nu X$	4 nb	0.8 Hz	high	~ 45	~ 45	none
$p\bar{p} \rightarrow ZX \rightarrow b\bar{b}X$	1 nb	0.2 Hz	~ 45	low	~ 0	~ 5
$p\bar{p} \rightarrow t\bar{t} \rightarrow \ell + (b)\text{jets}$	2.5 pb	1.8/hour	~ 50	~ 45	~ 50	~ 5
$p\bar{p} \rightarrow tX$ (s-chan)	1 pb	0.7/hour				
$p\bar{p} \rightarrow tX$ (t-chan)	1 pb	1.4/hour				
$p\bar{p} \rightarrow WH \rightarrow \ell\nu b\bar{b}$	26 fb	0.4/day	~ 45	~ 45	~ 45	~ 5
$p\bar{p} \rightarrow ZH \rightarrow \nu\nu b\bar{b}$	22 fb	0.4/day	~ 45	none	~ 70	~ 5

partons then hadronize to produce the particles observed in the detector.

Such QCD processes are referred to as “low- P_t ” because the transverse momenta of the objects produced in the hard scatter tend to have P_t ’s small compared to the beam energy. More rare events, such as vector boson, top quark and Higgs production as well as signals of physics beyond the standard model are called “high- P_t ” because they contain objects with relatively large P_t .

Also present in any hard scattering event at the Tevatron are the remnant partons of the proton and antiproton, which also hadronize to form jets of particles, referred to as the “underlying event”, traveling basically along the beam direction. Occasionally, some of the particles from the underlying event are produced with relatively large transverse momenta and contaminate the products of the hard scattering, confusing event classification.

An idea of the problems and opportunities facing those physicists studying high P_t physics at the Tevatron can be obtained by examining the first three columns of Table 3. Event rates are high enough that we will be able to record significant samples of some of the most interesting physics processes. However, the QCD multi-jet cross-section is huge – 10 orders of magnitude higher than top production, for example.

As mentioned before, production of relatively low energy jets by QCD at these

energies is a well understood process (although other aspects of QCD observable at the Tevatron are much more interesting). These events are therefore a major obstacle to getting at the physics we don't understand, such as that associated with the breaking of the electro-weak symmetry. The first step in overcoming this obstacle is to write interesting events to tape for offline analysis at a later stage. Obviously, it is impossible to do this at the 10 MHz rate of QCD events. So sophisticated selection mechanisms must be developed to winnow the few interesting events that occur on a time scale of seconds to hours from the overwhelming QCD background, all at a frequency set by the $p\bar{p}$ bunch crossing time of 396 ns. This daunting task is the job of the trigger system, which is therefore one of the most critical elements in the experiments at the Tevatron.

Offline, even more sophisticated algorithms are required to produce clean samples of signal events with well-understood detector effects and low background levels. This often requires choosing specific event topologies for study, which also impacts the trigger algorithms developed to select these events online. For example, decays of vector bosons to quarks strongly resemble QCD events, so only decays to leptons are generally used (see Figure 3 for a representative Feynman diagram). The top quark decays nearly 100% of the time via $t \rightarrow bW$. Again, leptonic decays of the W (for at least one of the tops in the event) tend to give the cleanest event samples. An example is given in Figure 3. Finally, Higgs production at the Tevatron occurs mainly via gluon-gluon fusion (through a top-quark loop) with the Higgs then decaying either to $b\bar{b}$ (for Higgs mass less than about 130 GeV) or to vector boson pairs (for higher Higgs masses). While leptonic decays of the vector bosons be used to identify Higgs events in this production mode for high mass Higgses, the $b\bar{b}$ final state seen in low mass Higgs production is swamped by QCD produced $b\bar{b}$ pairs. This forces us to search for a low mass Higgs in its associated production mode

$$p\bar{p} \rightarrow H + W(Z) \rightarrow b\bar{b} + \ell\nu, qq'(\ell\ell, \nu\nu, qq)$$

even though the cross-section for this is lower by almost an order of magnitude than that for the gluon-gluon mode. Feynman diagrams for low mass Higgs production are given in Figure 4.

Luckily for trigger algorithm developers and offline analyzers, it turns out that these interesting physics channels share a reasonably small number of simple event characteristics that allow them to be distinguished from QCD background. These characteristics all arise from two general features of QCD events at hadron colliders contrasted to other (electro-weak) physics processes.

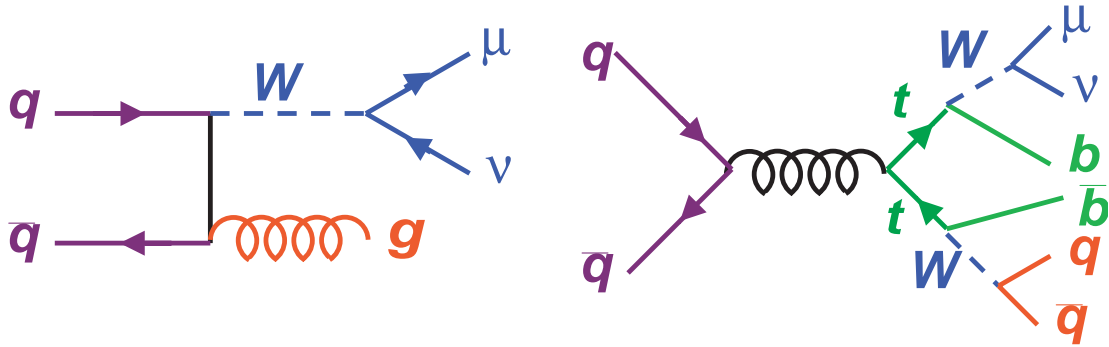


Fig. 3. Feynman diagrams for W production with $W \rightarrow \mu\nu$ (left-side) and top pair production with one top decaying semi-leptonically and the other decaying hadronically (right-side).

1. The energy scales of the QCD hard scatter is set by the energy distribution of partons within the p and \bar{p} , which are peaked at low values. This means that jets (and their component particles) in QCD events tend to have energies that are low compared to the beam energy. In contrast, energy scales in the production of such objects as weak bosons, top, Higgs and beyond the SM particles are set by the heavy mass of the primary particle produced. Decay products of these particles then share their high energies. B-physics events tend to have energies intermediate between these two extremes as set by the b -quark mass.
2. Hadronization of final-state partons from QCD hard scattering favors the production of low mass mesons and baryons containing light quarks (u, d, s). If unstable, these particles tend to have either very short lifetimes (strong or EM) or very long lifetimes. In addition, their low energy means that they do not produce high P_t leptons or neutrinos in their decays. The heavy particles discussed above, however, can decay to high P_t leptons or neutrinos. They also often have b -quarks in their decay chains. These quarks produce B hadrons with lifetimes such that they travel several mm's in the detector before decaying – topologies that are reconstructible using precise tracking information from silicon detectors.

Based on these differences, a short list of distinguishing variable can be constructed that allow other physics processes to be distinguished from QCD. These are shown below and typical values for some of them are listed in Table 3.

1. Jet transverse energy – E_t^{jet}

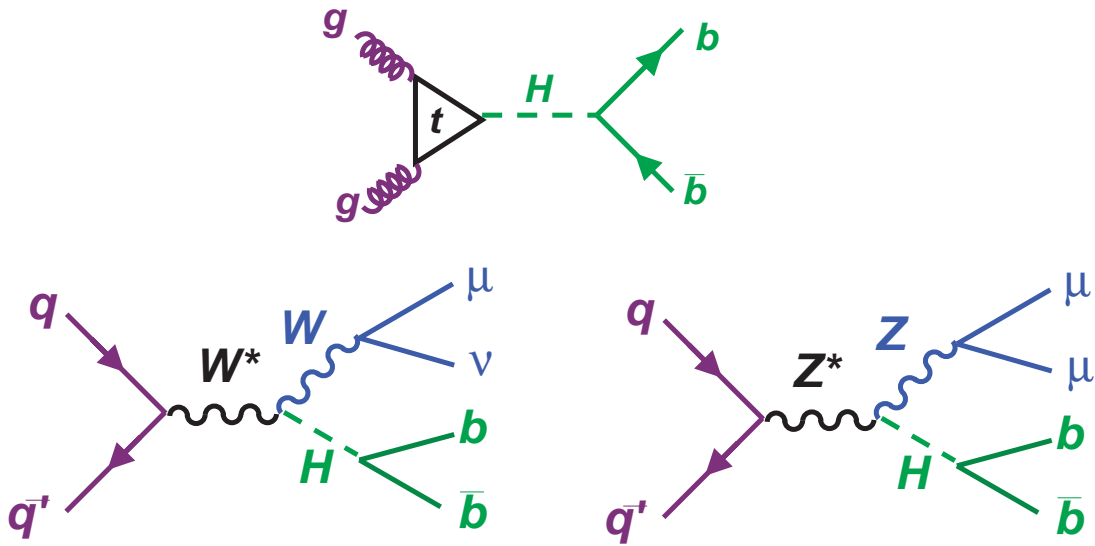


Fig. 4. Feynman diagrams for Higgs production through gluon fusion (top diagram) and associated Higgs production with W 's and Z 's (bottom diagrams).

2. Lepton transverse energy – E_t^{lept}
3. Missing transverse energy – ME_t . This can be caused by the presence of high P_t neutrinos, or other non-interacting particles, that are not detected and therefore spoil the energy balance of the event in the transverse plane.
4. Multi-particle vertices that are displaced from the point at which the $p\bar{p}$ interaction happened – Displaced Vertices. Such vertices can arise from the decay of moderately long-lived B -hadrons that are produced at the interaction point.
5. High energy photons

These variables, and others derived from them, form the basis for most of the trigger and offline algorithms used at CDF and DØ.

4 First Results and a Look into the Future

Having seen what the Run II capabilities are and generally how physics is done at the Tevatron, we now turn our attention to the actual CDF and DØ results. As mentioned before, only a small amount of data had been analyzed at the time of the SLAC Summer Institute (10–20 pb^{-1}) so the results discussed here, which are all preliminary, give only

a taste of what can be done. We will, therefore, also examine what *can* be done with Run II data set, with special attention paid to analyses to watch in the coming years.

An enormous amount of work has gone into preparing these results and predictions and justice certainly cannot be done to their beauty and complexity in a few pages. Interested readers are encouraged to visit the web sites of CDF⁸ and DØ⁹ for up to the minute information about the experiments. The preliminary results presented here were all prepared for the ICHEP conference in Amsterdam. More details on them can be found in specific talks and writeups (there were 21 from the Tevatron) linked off of the ICHEP02 web page.⁷ Summaries were given by F. Bedeschi¹⁰ and M. Narain.¹¹ Finally, predictions of CDF and DØ sensitivities were taken mainly from the Run II Tevatron Physics Working Groups¹² and also from some of the results presented at the 2001 Snowmass workshop.¹³

One final note: B-physics at the Tevatron will not be discussed in the following as it is extensively covered by F. Würthwein in his contribution to this conference⁵ and in the Run II B-Physics Working Group Report.¹⁴

4.1 QCD

Although QCD events have been discussed mainly as background to other physics processes many important studies of the strong force will be performed at the Tevatron in Run II. Among these are tests of (Next-to-)Next-to-Leading-Order, (N)NLO, QCD using weak boson P_t distributions and the angular distribution of leptons from W decays. Previous measurements of these distributions are statistics limited and much more precise measurements should be possible in Run II. Direct photon production will also be used to test QCD and to measure the gluon distribution in the proton where previous results are inconsistent. Searches for deviations between data and predictions for well understood QCD distributions, such as the di-jet invariant mass distribution, can also be used to detect evidence of physics beyond the SM. Finally, diffractive physics, such as studies of the properties of the pomeron should also prove to be a rich field in Run II.

Aside from these important physics topics, QCD remains a large background for many other analyses. It must therefore be thoroughly understood before precise results can be obtained. Some of the issues that will be addressed here in Run II are more precise tuning of Monte Carlo event generators, better measurements of parton distribution functions using W P_t distributions, direct photon data and high E_t jet data, and

developing a better understanding of the properties of various jet-finding algorithms.

Work has already begun on many of these topics and first physics distributions were shown at the ICHEP02 conference.¹⁵ As an example of the work shown, DØ has produced preliminary jet P_t spectra and di-jet invariant mass spectra for events in two $|\eta|$ regions (see Figure 5). Although these distributions use preliminary values for the jet energy scale and are not fully corrected, they still show evidence of events with jet $P_t > 400$ GeV, which is an interesting region both for parton density measurements and new physics searches. CDF has also made great strides, showing the first comparison of three-jet production with a NLO QCD prediction at a hadron collider. Agreement between the data and the NLO QCD prediction for the Dalitz variables $x_i = 2E_{jet-i}/m_{3-jet}$ is quite good (see Figure 6). The measured, total three-jet cross section in the kinematically allowed region, $466 \pm 2_{-71}^{+206}$ pb also agrees well with the prediction of 402 ± 3 pb.

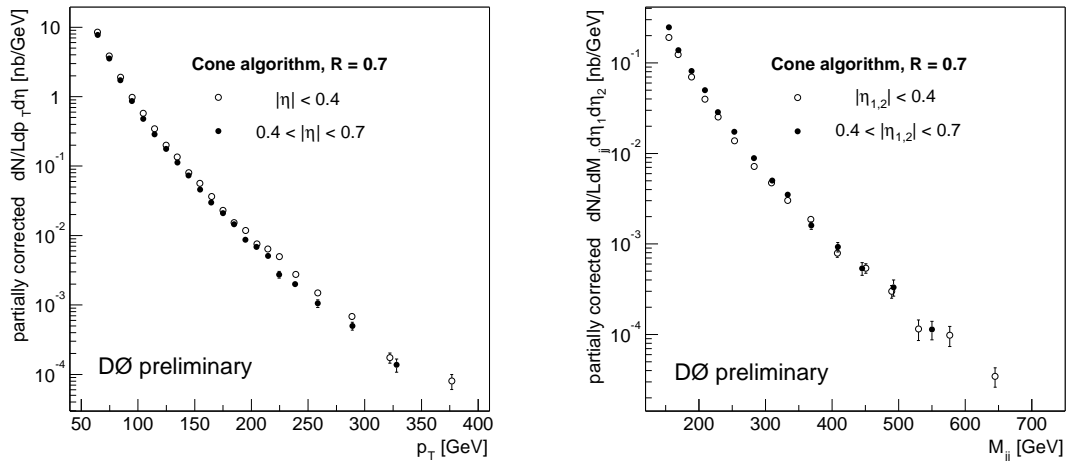


Fig. 5. DØ preliminary inclusive jet P_t distribution (left plot) and di-jet invariant mass spectrum (right plot).

4.2 W/Z Boson and Top Physics

Run II is expected to produce significant advances in our understanding of the properties of the W and Z bosons and the top quark. As can be seen from Table 4, event yields for these particles in Run II will be orders of magnitude more than those in Run I. This will allow large improvements in precision on existing measurements as well

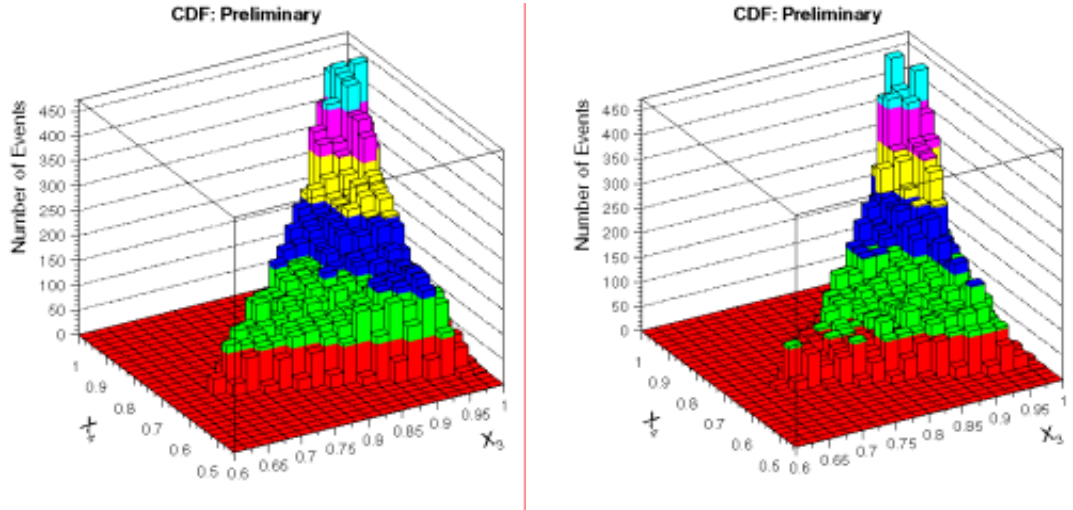


Fig. 6. Preliminary Dalitz distributions of CDF 3-jet data (left plot) and NLO QCD prediction (right plot).

as opening up some new areas of study. A summary of some of the most interesting electro-weak measurements in Run II, compared to Run I results and expectations from the Large Hadron Collider (LHC), are also given in Table 4.

Several topics deserve specific note. Measurement of the forward-backward asymmetry in $Z \rightarrow \ell^+ \ell^-$ events with the Run IIb data set will allow a determination of the $\sin^2 \theta_W$ to a precision comparable to the current world average. The precision on the mass measurement of the W and the top quark, for each experiment, will be improved to approximately 30 MeV and 3 GeV respectively in Run IIa. These variables are sensitive to the Higgs mass because of loop corrections. Comparing the Higgs mass value predicted from M_W , M_t and other electro-weak variables to the value that is found if the Higgs is observed will be a stringent test of whether the observed Higgs is as predicted in the SM. Measuring the decays of the top to a longitudinally polarized W and a b -quark will provide a test of the $V - A$ structure of the weak interaction in the top sector. Finally, a new area that will open up in Run II will be single-top production through W -boson exchange in the s - and t -channels. Feynman diagrams for these processes are shown in Figure 7. This will allow, for the first time, a direct measurement of the CKM matrix element $|V_{tb}|$. Predictions for the precision of these measurements compared to current and future values are given in Table 4.

CDF and DØ have produced first results on the road to these exciting measure-

Table 4. Expected event yields and measurement precisions for various W , Z and t -quark observables compared the current status and predictions from the LHC.

Measurement	Current	Run II / exp.		LHC (10 fb ⁻¹)
		(2 fb ⁻¹)	(15 fb ⁻¹)	
reconstr. $W \rightarrow \ell \nu$	77k	2300k	17250k	6×10^7
reconstr. $Z \rightarrow \ell^+ \ell^-$	10k	202k	1515k	6×10^6
reconstr. $p\bar{p} \rightarrow t\bar{t} \rightarrow \ell + \text{jets}$	~ 20	~ 800	~ 6000	8×10^5
reconstr. $p\bar{p} \rightarrow tX$	0 (Ref. 16)	~ 150 (Ref. 16)	~ 1200	1.7×10^4 (Ref's 18,19)
$\delta \sin^2 \theta_W$	5.1×10^{-4} (Ref. 20)	4×10^{-4} (Ref. 21)		1.4×10^{-4} (100 fb ⁻¹) (Ref. 21)
δM_W [MeV]	39	27	17	10
δM_t [GeV]	5.1 (Ref. 22)	2.7 (Ref. 23)	1.3	< 2 (Ref's 18,19)
$\delta M_H / M_H$ [%] (Ref. 23)	58	35	25	18
$\delta BR(t \rightarrow W_o b)$ [%]	42 (Ref. 24)	9 (Ref. 17)	4	1.6 (Ref. 19)
$\sigma(p\bar{p} \rightarrow tX)$ V_{tb}	< 13.5 pb — (Ref. 25)	20% 12% (Ref. 17)	8% 5%	$< 5\%$ (100 fb ⁻¹) (Ref. 19)

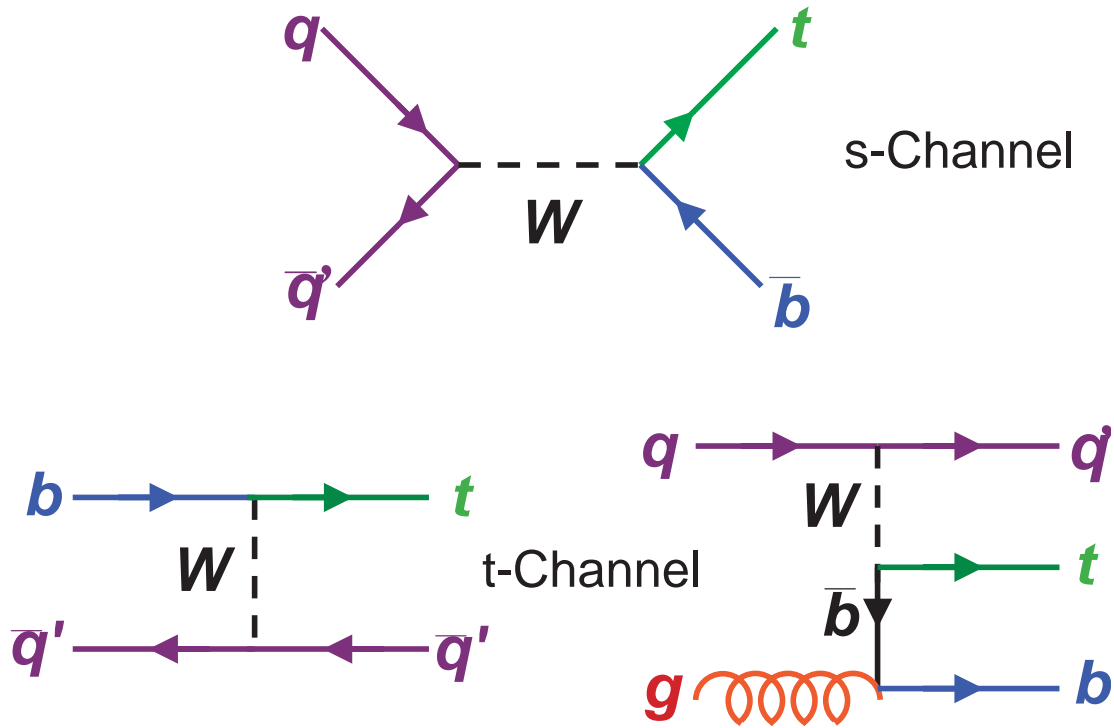


Fig. 7. Feynman diagrams for single top production in the s - and t -channels.

ments.^{16,17} Hundreds of $Z \rightarrow \ell^+ \ell^-$ and thousands of $W \rightarrow \ell \nu$ events have been observed (see Table 5) and CDF has even observed a $W \rightarrow \tau \nu$ signal as an excess of one- and three-track jets (most τ decays have one or three charged particles) in events with narrow jets consistent with $W \rightarrow \tau \nu$ production (see Figure 8). First measurements of cross-section times branching ratio have also been made for both W and Z production in the electron and muon channels as shown in Table 5 and Figure 9. These measurements are quite consistent with theoretical predictions and show clearly the evolution of the cross-section with energy when compared with previous measurements.

A preliminary measurement of the W width has also been made by both collaborations using the ratio of the W to Z cross-section times branching ratio measurements (see Table 5). This technique relies on input from LEP for the $Z \rightarrow e^+ e^-$ branching ratio and from theory for a prediction of the W/Z cross-section ratio and is not the ultimate method that will be used to determine this quantity using Run II data. However the good agreement with the theoretical prediction is an indication that we are on the right track to making competitive measurements using W 's and Z 's.

Preliminary results for other production properties of vector bosons are also being

Table 5. Numbers of candidate W and Z events in the electron and muon decay channels observed by CDF and DØ. Also shown are preliminary measurements of W and Z production cross-section times branching ratio measurements with errors from event statistics, systematics and the luminosity measurement, in that order.

Channel	Candidates		$\sigma \times BR$ [pb]	
	CDF	DØ	CDF	DØ
$W \rightarrow e\nu$	5547	9205	$2600 \pm 30 \pm 130 \pm 260$	$2670 \pm 60 \pm 330 \pm 270$
$Z \rightarrow e^+e^-$	798	328	—	$266 \pm 20 \pm 20 \pm 27$
$W \rightarrow \mu\nu$	4561	—	$2700 \pm 40 \pm 190 \pm 270$	—
$Z \rightarrow \mu^+\mu^-$	~ 170	~ 57	—	—
Γ_W [GeV]	2.118 ± 0.042^{22} (world ave)		$1.67 \pm 0.24 \pm 0.14$ (\pm stat,syst)	$2.26 \pm 0.18 \pm 0.29 \pm 0.04$ (\pm stat,syst,theory)

made. CDF has produced a first distribution of the forward-backward asymmetry vs e^+e^- invariant mass for $Z \rightarrow e^+e^-$ events. Remember, that this can be used to determine $\sin^2 \theta_W$. Although statistics are still limited, the data agrees quite well with theoretical expectations as can be seen in Figure 10.

On the top quark side, DØ has begun the process by examining W +jets events. These are interesting for many analyses, with top events inhabiting the $W+\geq 3$ -jets sample and Higgs possibly showing up in $W/Z+\geq 2$ -jets. Although statistics are still too low to have observed any top events (let alone the elusive Higgs) the DØ data shown in Figure 11 indicate that we have made a strong start.

4.3 The Higgs

One of the most exciting prospects for Run II at the Tevatron is the possibility of discovering the Higgs. The opportunity is evident from an examination of Figures 12 and 13. Figure 12, which is the LEP Electroweak Working Group fit of the Higgs mass to precision electro-weak observables,²⁰ indicates that, if the Higgs is SM-like, it should be light. The fit gives $M_H = 81_{-33}^{+52}$ GeV, or $M_H < 193$ GeV at 95% CL, which is compatible with direct searches at LEP II²⁶ that limit this range to $M_H > 114.4$ GeV at 95% CL. A light Higgs is also required by the minimal supersymmetric extension to the SM, which restricts the lightest Higgs mass to be less than approximately 135 GeV. All of this is good news for the Tevatron, as can be seen from Figure 13. Given the

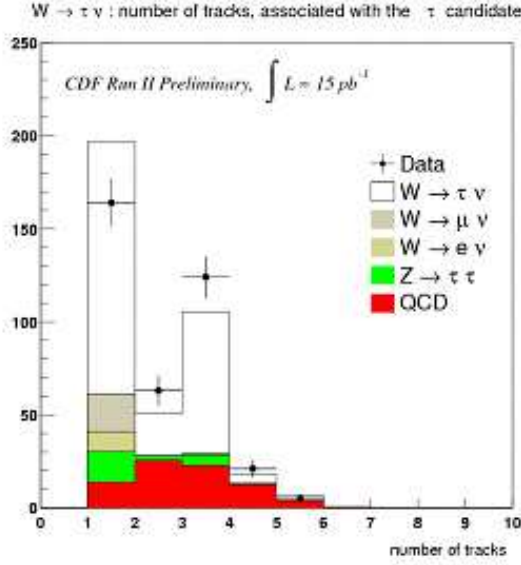


Fig. 8. Track multiplicity in the τ -candidate jet for the CDF $W \rightarrow \tau \nu$ selection.

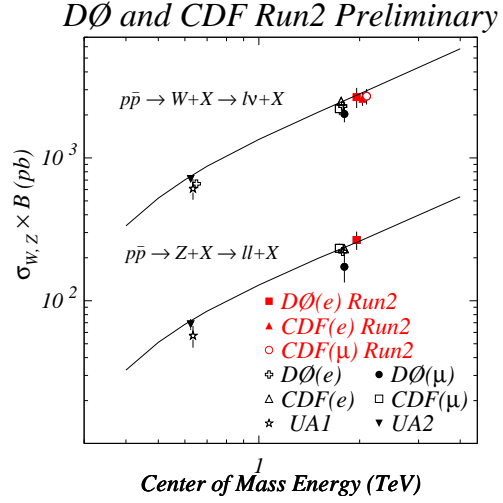


Fig. 9. A comparison of the Run II CDF and DØ measurements of the W and Z production cross-sections times leptonic branching ratios at $\sqrt{s}=1.96\text{TeV}$ with previous measurements and theoretical predictions.

luminosities hoped for in Run IIb, we should be able to see 3σ evidence for an SM-like Higgs up to masses of about 180 GeV.

To accomplish this feat, however, information from all Higgs production and decay modes must be used.

- $M_H < 130 \text{ GeV}$: $q\bar{q}' \rightarrow W/Z H \rightarrow \ell\nu b\bar{b}, \nu\bar{\nu} b\bar{b}, \ell^+\ell^- b\bar{b}, q\bar{q}b\bar{b}$
- $M_H > 130 \text{ GeV}$: $gg \rightarrow H \rightarrow W^+W^-/Z/Z \rightarrow \ell^+\ell^-\nu\bar{\nu}, \ell^+\ell^-\text{jj}, \ell^+\ell^-\ell'^+$

Nearly all aspects of the detectors will be used in these searches. However, triggers, particularly those involving leptons and jets+ ME_t , will need to be nearly 100% efficiency for Higgs events, and b -quark identification will have to be superb – with tagging efficiencies of 60–75% and $b\bar{b}$ resonance mass resolution of $\sim 30\%$ required.

The game is particularly intense because the LHC experiments should be able to see nearly any type of Higgs within a year of their start. This has motivated CDF and DØ to start looking at Higgs signatures even though several years worth of accumulated luminosity will be required before even the LEP limits can be passed. DØ has started the process by looking for events containing e^+e^- and ME_t (Ref's 16,17). Excesses of

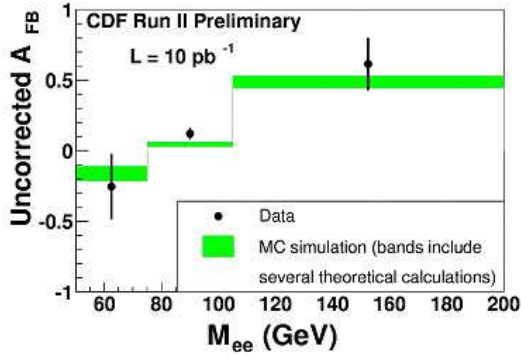


Fig. 10. The forward-backward asymmetry as a function of e^+e^- invariant mass for $Z \rightarrow e^+e^-$ events from CDF.

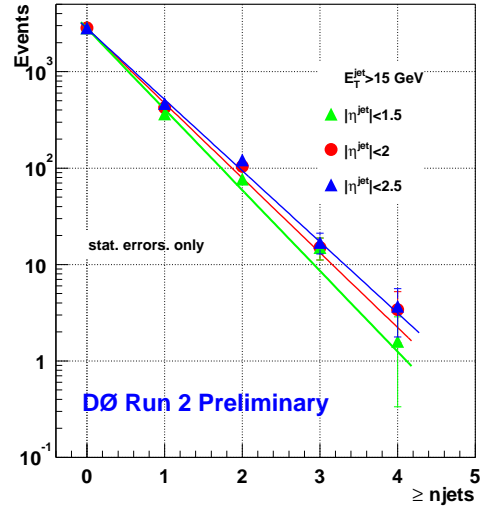


Fig. 11. The DØ measurement of $W(\rightarrow e\nu)+\text{jets}$ vs. number of reconstructed jets.

such events over SM backgrounds are predicted in models where the Higgs coupling to fermions is suppressed. In these cases the branching ratio of $H \rightarrow W^+W^-$ is $\sim 98\%$ for $M_H > 100\text{GeV}$. Preliminary results from DØ are shown in Figure 14. No excess above predicted backgrounds is observed with the 9pb^{-1} analyzed. Even though no signal is observed this study is important in that it increases confidence in our ability to model backgrounds to Higgs production.

4.4 Beyond the Standard Model

The limitations of the SM lead most physicists to believe that it cannot be the whole story behind the fundamental forces of nature. Unfortunately, no evidence for any chink in the armor of the SM has yet been found, although a bewildering array of theoretical models have been proposed to address the SM's shortcomings (see Ref's 27-31). Because of the excellent detector capabilities and the large data set, Run II should be a fruitful field in which to search for signals of physics beyond the SM.

Sensitivities for a sample of new physics topics are shown in Table 6. While this list shows only the tip of the new physics iceberg, it does give a sense of the capabilities of the Tevatron in beyond the SM searches. A few comments about the entries in the list are in order.

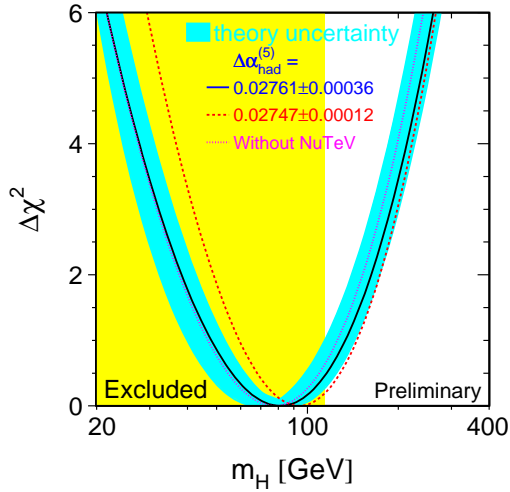


Fig. 12. $\Delta\chi^2$ curve for the fit of the Higgs mass to precision electro-weak data.²⁰

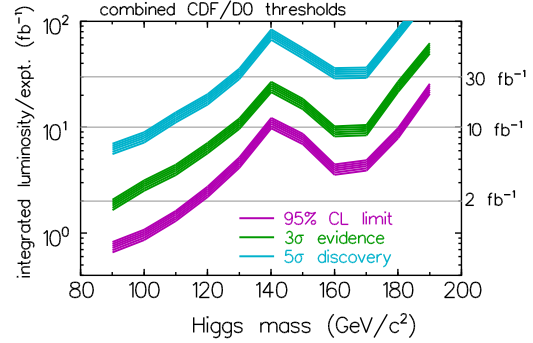


Fig. 13. Predictions of Higgs sensitivity vs. mass for Run II.²⁷

Given the *ad hoc* nature of electro-weak symmetry breaking in the SM, several theoretical frameworks have been developed to attempt to explain it. One example is *supersymmetry*, or *SUSY*,³² which postulates superpartners having particles with spins differing by one half a unit from all known SM particles as well as an extended Higgs sector containing five physical Higgs states. In its raw state, SUSY contains more than 100 parameters allowing it to predict almost any type of new phenomenon that could be observed. This situation can be improved (from an experimentalist's point of view) by making various, well motivated, assumptions about relationships between parameters. Different types of assumptions lead to different versions of SUSY, one of the most popular of which is the Minimal Supersymmetric Standard Model, or MSSM, where only five parameters are required to describe the model. (See Ref. 27 for a good overview.)

Another possibility is *technicolor*,³³ which breaks electroweak symmetry when the interactions of an extended gauge symmetry containing extra multiplets of technifermions become strong. Still another option lies in theories with large extra dimensions,³⁴ which solves the problem of the disparity between the Planck scale at which gravity is strong and the electro-weak scale by assuming that the natural energy scale of gravity, (M_S) actually *is* near the electro-weak scale. This assumption is made plausible by postulating the existence of extra spatial dimensions in which gravity also acts,

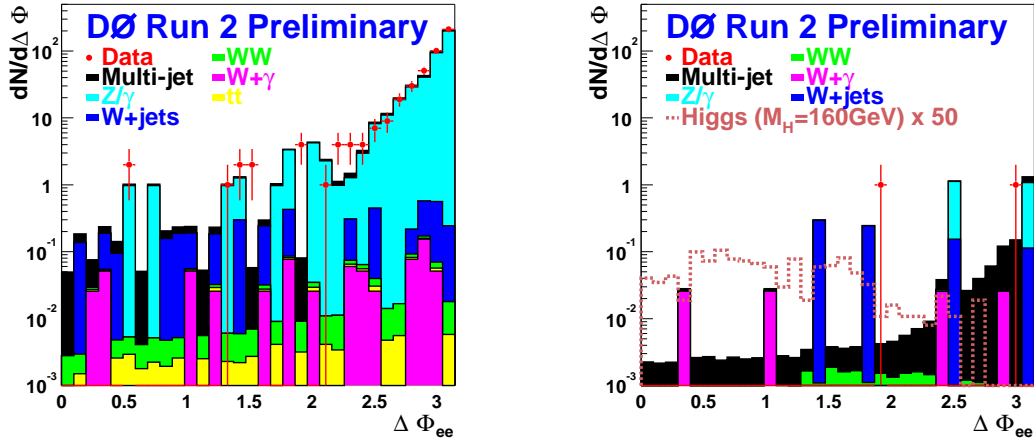


Fig. 14. The e^+e^- azimuthal opening angle in the DØ $H \rightarrow WW \rightarrow e^+e^-\nu\bar{\nu}$ search. The left plot shows data containing good e^+e^- pairs while the right plot shows the distribution after all selection cuts (large ME_t , no jets, etc.).

and leads to the prediction of a number of new graviton states with various couplings to fermions and bosons. Other theories predict an enhancement in the rate of decays of the top quark that are highly suppressed in the SM³⁵ or the existence of heavier versions of the W - and Z -bosons.³⁶

As can be seen from Table 6, the precision with which all of these theories (and many more) can be tested will be substantially improved in Run II at the Tevatron.

First attempts at searching for new physics signals have already been made by the DØ collaboration.⁴⁴ Gauge mediated models of supersymmetry can give scenarios where the lightest supersymmetric particle is the gravitino (the partner of the graviton) and the next to lightest supersymmetric particle is a neutralino, χ_1^0 (one of the partners of the neutral gauge bosons and Higgses) or a slepton (one of the lepton partners). These lead to decay modes of the type:

$$p\bar{p} \rightarrow \text{gauginos} \rightarrow W/Z/\gamma + \chi_1^0 \chi_1^0 \rightarrow \gamma\gamma + \tilde{G}\tilde{G} + X.$$

The gravitinos, \tilde{G} , do not interact in the detector and are detected as missing energy. Results of the search are shown in Figure 15. Although the sensitivity with the $\sim 10 \text{ pb}^{-1}$ collected so far is too small to exclude any of the SUSY parameter space, an approximately model independent lower limit for the cross-section of this process has been set at 0.9 pb.

Table 6. A selection of new physics sensitivities at the Tevatron in Run II compared to the current state of knowledge and LHC expectations.

Model	Current Excl.	Sensitivity	
		Run IIb	LHC (100fb ⁻¹)
MSSM ($\tan \beta, M_A$)	$0.5 < \tan \beta < 2.4$ (Ref. 37)	\sim all 5σ (Ref. 27)	all
Technicolor ($M_{\rho T8}$ [GeV])	> 600 (Ref. 39)	> 850 (2fb ⁻¹ , Ref. 39)	$\gg 800$ (Ref. 38)
Extra Dim. (M_S [TeV])	$> 1.0-1.4$ (Ref. 39)	$2.1-3.5$ (Ref. 40)	$6-9$ (Ref. 41)
Rare Top ($t \rightarrow qZ$) ($t \rightarrow q\gamma$)	$< 33\%$ $< 3.2\%$ (Ref. 42)	2×10^{-3} 2×10^{-4} (Ref. 17)	2×10^{-4} 3.4×10^{-5} (Ref. 19)
New bosons ($M_{Z'}$ [GeV])	> 690 (Ref. 39)	$900-1200$ (Ref. 39)	5000 (Ref. 43)

Another possibility for extensions of the SM is lepto-quark models, where new particles exist that carry both quark and lepton quantum numbers. DØ has searched for such particles in the 2-electron + 2-jet channel, unfortunately with no success (see Figure 16). This allows a limit on the presumed lepto-quark mass of, $M_{LQ} > 113$ GeV to be set at the 95% CL (assuming the branching ratio to this mode is 1).

Finally, DØ has also looked for gravitons arising in theories with large extra dimensions. Such particles can decay to e^+e^- or $\gamma\gamma$ and interfere with the SM production mechanisms for these final states. A two-dimensional distribution of diEM (electrons and photons are not distinguished) invariant mass vs. the cosine of the scattering angle in the center-of-mass frame of the hard scatter is shown in Figure 17. Again, the data distribution is indistinguishable from the SM prediction allowing a limit on the fundamental scale of gravity to be set at $M_S > 0.82$ TeV, in Hewett's convention.⁴⁵ This compares favorably with the limit set in the DØ Run I search – $M_S > 1.2$ TeV (Ref. 46).

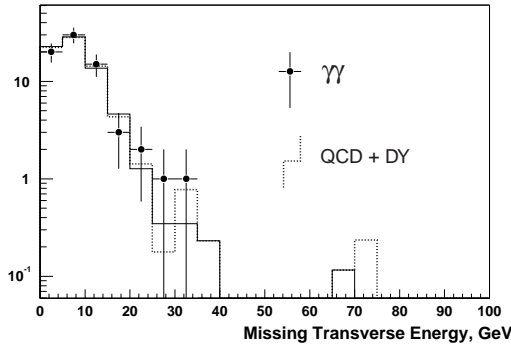


Fig. 15. Preliminary DØ results for a gauge mediated SUSY search. Show is the distribution of missing E_t in $\gamma\gamma$ events.

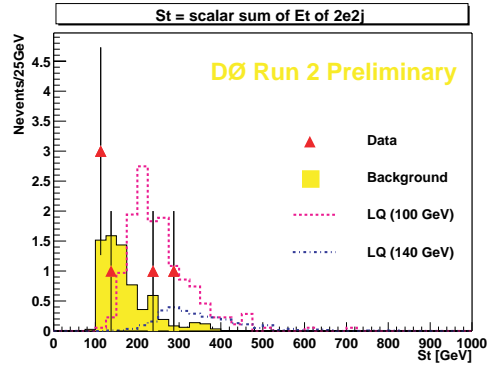


Fig. 16. Distribution of the scalar sum of E_t seen in the DØ detector for $eejj$ events.

5 Conclusions

From QCD studies, to electro-weak precision measurements, to probes of CP violation and searches for as-yet undiscovered particles, the Run II physics menu is full of interesting topics. We have seen that world-best levels sensitivity are expected for a wide range of important measurements in Run II. First physics results presented at the ICHEP conference in July, 2002 indicate that we are well on the way to achieving these goals, with detector performances beginning to approach design specifications and sophisticated analysis techniques being tuned up. Of course, with such an exciting program, things are not standing still at Fermilab. Accelerator and detector performances are continuing to improve. In fact, with the steady running we have enjoyed through the fall we should have a data sample of 50 pb^{-1} or more by the end of the year and conceivably 250 pb^{-1} (more than twice the Run I sample) in time for the summer. Further in the future, a new series of upgrades to the machine and the detectors should allow us to collect 15 fb^{-1} by the time LHC starts up. With data sets of this size, a low mass Higgs is well within our grasp. The best is clearly yet to come!

6 Acknowledgments

I would like to acknowledge all of the CDF and DØ speakers at ICHEP from whom I stole material shamelessly. I also profited from the good advice of B. Ashmanskas, G. Blazey, G. Brooijmans, J. Dittmann, Y. Gershtein, A. Goshaw, J. Houston, J. Krane,

G. Landsberg, N. Lockyer, M. Narain, G. Steinbrück, J. Womersley and S. Worm. Finally, I am happy to thank the SLAC Summer Institute organizers for providing such a stimulating conference, and for putting up with all my last-minute requests.

References

- [1] “What I tell you three times is true”
from *The Hunting of the Snark*, by Lewis Carroll.
- [2] For a review see, J. Hewett, *The Standard Model and Why We Believe It*,
hep-ph/9810316.
- [3] For a review see, W. Bernreuther, *CP Violation and Baryogenesis*,
hep-ph/0205279.
- [4] F.Abe, *et al.* (CDF), Phys. Rev. Lett. **74**, 2626 (1995).
S.Abachi, *et al.* (DØ), Phys. Rev. Lett. **74**, 2632 (1995).
- [5] F. Würthwein, *B Physics Studies at the Tevatron*, these proceedings.
- [6] See the *Run II Handbook*, available at
<http://www-bd.fnal.gov/runII/index.html>
for a more detailed description.
- [7] *International Conference on High Energy Physics*, July 24-31, 2002, Amsterdam,
the Netherlands, <http://www.ichep02.nl>.
- [8] Information about the CDF detector, collaboration and physics results can be
found in the CDF WWW pages: <http://www-cdf.fnal.gov/>.
- [9] Information about the DØ detector, collaboration and physics results can be found
in the DØ WWW pages: <http://www-d0.fnal.gov/>.
- [10] F. Bedeschi, *First CDF Run II Results*,
talk presented at the *International Conference on High Energy Physics*, July 24-
31, 2002, Amsterdam, the Netherlands,
- [11] M. Narain, *Results from the DØ Experiment at the Tevatron*,
talk presented at the *International Conference on High Energy Physics*, July 24-
31, 2002, Amsterdam, the Netherlands,
- [12] Information about all the Tevatron Run II Working Groups can be found off of the
Fermilab theory group web page: <http://theory.fnal.gov/>.

- [13] See the Snowmass web page: <http://snowmassserver.snowmass2001.org>.
- [14] K. Anikeev, *et al.*, *B Physics at the Tevatron: Run II and Beyond*, hep-ph/0201071.
- [15] J. Dittman, *Photon and Jet Physics at CDF*, M. Zielinski, *Jet and Photon Physics at DØ*, talks presented at the *International Conference on High Energy Physics*, July 24-31, 2002, Amsterdam, the Netherlands,
- [16] D. Glenzinski, *Electroweak Prospects for Tevatron Run II*, talk presented at the *International Conference on High Energy Physics*, July 24-31, 2002, Amsterdam, the Netherlands,
- [17] I. Iashvilli, *Top Quark Physics at the Tevatron*, talk presented at the *International Conference on High Energy Physics*, July 24-31, 2002, Amsterdam, the Netherlands,
- [18] S. Haywood, *et al.*, *Electroweak Physics*, hep-ph/0003275.
- [19] M. Beneke, *et al.*, *Top Quark Physics*, hep-ph/0003033.
- [20] LEP Electroweak Working Group fits, M. Grünwald, *Electroweak Physics*, hep-ex/0210003.
talk presented at the *International Conference on High Energy Physics*, July 24-31, 2002, Amsterdam, the Netherlands,
- [21] U. Baur, R.K. Ellis and D. Zeppenfeld, *QCD and Weak Boson Physics at Run II* Fermilab-Pub-00/297.
- [22] K. Hagiwara, *et al.* (Particle Data Group), Phys. Rev. **D66**, (2002).
- [23] U. Baur, *et al.*, *Present and Future Electroweak Precision Measurements and the Indirect Determination of the Mass of the Higgs Boson*, hep-ph/0202001.
- [24] T. Affolder, *et al.* (CDF), Phys. Rev. Lett. **84**, 216 (2000).
- [25] D. Acosta, *et al.* (CDF), Phys. Rev. **D65**, 091120 (2002).
- [26] The LEP Working Group for Higgs Boson Searches, *Search for the Standard Model Higgs Boson at LEP*, LHWG Note/2002-01.
(<http://lephiggs.web.cern.ch/LEPHIGGS/www/Welcome.html>)
- [27] M. Carena, J.S. Conway, H.E Haber and J.D. Hobbs, *Report of the Tevatron Higgs Working Group*, hep-ph/0010338.

- [28] V. Barger, C.E.M. Wagner, T. Kamon, E. Flattum, T. Falk and X. Tata, *Report of the SUGRA Working Group for Run II at the Tevatron*, hep-ph/0003154.
- [29] S. Ambrosanio, *et al.*, *Report of the Beyond the MSSM Subgroup for the Tevatron Run II SUSY/Higgs Workshop*, hep-ph/0006162.
- [30] B. Allanach, *et al.*, *Searching for R-Parity Violation at Run II of the Tevatron* hep-ph/9906224.
- [31] R. Culbertson, S.P. Martin, J. Qiang and S. Thomas, *Low-Scale and Gauge-Mediated Supersymmetry Breaking at the Fermilab Tevatron Run II*, hep-ph/0008070.
- [32] J. Wess and J. Bagger, *Introduction to Supersymmetry, 2nd ed.*, (Princeton University Press, 1992);
H.P. Nilles, Phys. Rep. **110**, 1 (1984);
H. Haber and G. Kane, Phys. Rep. **117**, 75 (1985).
- [33] For a review see, *e.g.*, R.S. Chivukula, R. Rosenfeld, E.H. Simmons and J. Terning in, *Electroweak Symmetry Breaking and New Physics at the TeV Scale*, edited by T.L. Barlow, S. Dawson, H.E. Haber and J.L. Siegrist (World Scientific, 1996);
E. Eichten, K. Lane and J. Womersley, Phys. Lett. **B405**, 305 (1997);
K. Lane, Phys. Rev. **D60**, 075007 (1999).
- [34] N. Arkani-Hamed, S. Dimopoulos, G. Dvali, Phys. Lett. **B429**, 263 (1998).
- [35] G. Eilam, J. Hewett and A. Soni, Phys. Rev. **D44**, 1473 (1991).
Erratum, Phys. Rev. **D59**, 039901 (1999).
- [36] for a recent review see, A. Leike, Phys. Rep. **317**, 143 (1999).
- [37] The LEP Higgs Working Group, *Searches for the Neutral Higgs Bosons of the MSSM: Preliminary Combined Results Using LEP Data Collected at Energies up to 209 GeV*, hep-ex/0107030.
- [38] *ATLAS Detector and Physics Performance Technical Design Report*, LHCC 99-14/15 (1999).
(<http://atlas.web.cern.ch/Atlas/GROUPS/PHYSICS/TDR/access.html>)
- [39] W. Orejudos, *Minireview on Other Signatures of New Physics at the Tevatron*, talk presented at the *International Conference on High Energy Physics*, July 24-31, 2002, Amsterdam, the Netherlands.

- [40] K. Cheung and G. Landsberg, Phys. Rev. **D62**, 076003 (2000) (hep-ph/9909218).
- [41] D. Tovey, *Searches for New Physics at the LHC*, talk presented at the *International Conference on High Energy Physics*, July 24-31, 2002, Amsterdam, the Netherlands.
- [42] F. Abe, *et al.* (CDF), Phys. Rev. Lett. **80**, 2525 (1998).
- [43] T. Abe, *et al.*, *Linear Collider Physics Resource Book for Snowmass 2001, Part 3: Studies of Exotic and Standard Model Physics*, hep-ex/0106057. (<http://www.slac.stanford.edu/grp/th/LCBook/>)
- [44] G. Bernardi, *Minireview on Low-Scale Gravity and Extra Dimensions at HERA, LEP and the Tevatron*,
A. Connolly, *Search for MSSM Higgses at the Tevatron*,
V. Zutshi, *Search for SUSY at the Tevatron*,
talks presented at the *International Conference on High Energy Physics*, July 24-31, 2002, Amsterdam, the Netherlands.
- [45] J. Hewett, Phys. Rev. Lett. **82**, 4765 (1999).
- [46] B. Abbott, *et al.* (DØ), Phys. Rev. Lett. **86**, 1156 (2001).

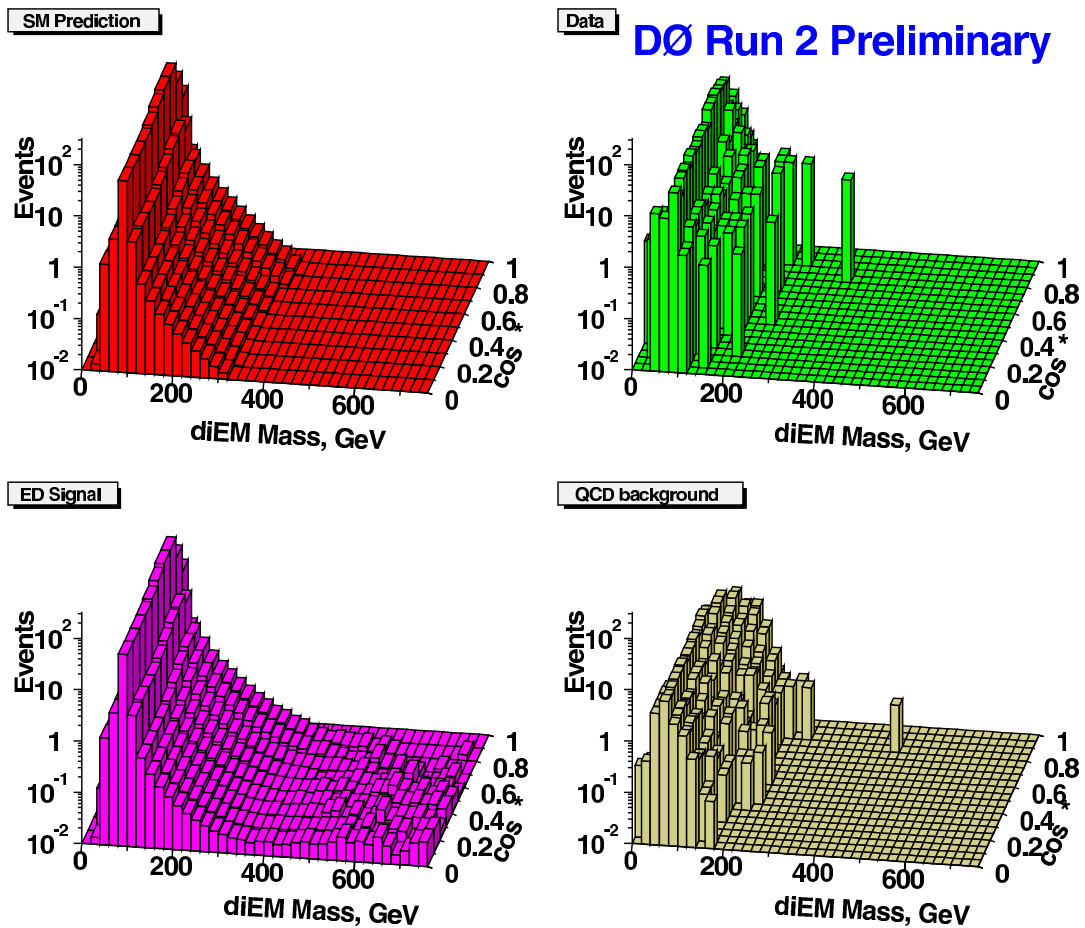


Fig. 17. Distributions of diEM invariant mass vs. center-of-mass scattering angle in the DØ large extra dimensions search. The SM prediction is shown in the upper-left, the DØ data in the upper-right, the prediction for an extra dimensions signal in the lower-left and the QCD background to the search in the lower-right.